Dalton Transactions

Accepted Manuscript

ROYAL SOCIETY OF CHEMISTRY

www.rsc.org/dalton

Cite this: DOI: 10.1039/c0xx00000x

www.rsc.org/xxxxxx

COMMUNICATION

A red phosphor $BaTiF_6:Mn^{4+}$: reaction mechanism, microstructures, optical properties, and applications for white LEDs

Xianyu Jiang, Zhen Chen, Shaoming Huang,* Jiaguo Wang and Yuexiao Pan*

Received (in XXX, XXX) Xth XXXXXXXXX 20XX, Accepted Xth XXXXXXXXX 20XX

DOI: 10.1039/b000000x

A red phosphor $BaTiF_6:Mn^{4+}$ with morphologies of micro rods and polyhedrons have been prepared respectively by etching TiO_2 and $Ti(OC_4H_9)_4$ in HF solution with optimized concentration of $KMnO_4$ at 1.5 mmol/L in hydrothermal condition. Red phosphor $BaTiF_6:Mn^{4+}$ exhibits a broad excitation band in blue and sharp emission peaks in red. White LED (WLED) fabricated with red phosphor $BaTiF_6:Mn^{4+}$ shows "warm" white light that possesses color rendering index of 93.13 at color temperature 4073.1 K.

1. Introduction

In recent years, special attention has been given on the synthesis of phosphors with broad absorption band in 380~490 nm, which show potential applications in WLEDs.[1-5] The WLEDs fabricated with blue semiconductor and yellow phosphor have poor color rendering because of the scarcity of red components in their spectra.[6,7] It is feasible to obtain "warm" white light with high color rendering (>80) and low color temperature (<4000 K) by mixing a red phosphor into packages of WLEDs.[8-10]

The red phosphors for application in WLED coated with YAG:Ce should have a strong absorption in blue and an intense emission in red. Conventional red phosphors, such as Eu^{3+} doped inorganic compounds, possess high quantum efficiency but the excitation band of Eu^{3+} in blue region is too narrow due to 4f - 4f transitions of Eu^{3+}.[11-14] From a spectroscopic point of view, Eu^{2+} doped sulfides and nitrides can meet the requirements for LEDs applications. However, the poor chemical stability of sulfides and critical synthetic requirements of air-sensitive metal nitrides make them unfavorable candidates for competitive products.[5,15-17]

Mn^{4+} doped red phosphors have received increasing attentions due to their broad absorption band in 380~490 nm and sharp emission peaks at 610~760 nm.[18-26] Among them, Mn^{4+} doped dialkli hexafluorometallates in the form of $A_2XF_6:Mn^{4+}$ (A = K, Na, and Cs; X = Si, Ge, Zr, and Ti) are especially attractive due to their maximum absorption band in blue (that matches well with the electroluminescence of InGaN chip) and sharp emission peaks in red (that possesses high color purity), which shows significant potential application on WLEDs. The WLEDs show "warm" white light with a high color rendering 90 at color temperature 3088 K by coating a red phosphor $K_2TiF_6:Mn^{4+}$ together with yellow YAG:Ce phosphor on InGaN chip.[18]

The red phosphor $BaTiF_6:Mn^{4+}$ was obtained from TiO_2, $BaCO_3$ and $K_2[MnF_6]$ by evaporation of the reaction mixture to dryness but detailed information such as the concentrations and the reaction temperatures are not provided.[25] Adachi's group reported the photoluminescence and Raman scattering spectroscopies of $BaTiF_4:Mn^{4+}$ prepared by two-step method: first, pure $BaTiF_6$ powder was synthesized from a mixed solution of HF, H_2SiF_6, H_2O, BaF_2, and titanium sponge; second, the red phosphor $BaTiF_6:Mn^{4+}$ was obtained by dipping $BaTiF_6$ powder in a mixture of HF, H_2O, and $KMnO_4$ for about 6 h.[26] However, The phase $BaSiF_6$ should be formed by reaction of H_2SiF_6 and BaF_2, and $BaTiF_6:Mn^{4+}$ also shows red luminescence.[26] The concentrations of $KMnO_4$ plays an important role to obtain pure phase of red phosphor such as $BaSiF_6:Mn^{4+}$ free of MnO_2 in our previous work[27] but no information about the concentration of HF and $KMnO_4$ was provided in the reported work about $BaTiF_6:Mn^{4+}$.[25,26] In some previous reported works, HF-rich and $KMnO_4$-rich solutions, expensive metals (such Ge, Ti, Zr) are generally needed for synthesis of red Mn^{4+} doped dialkli hexafluorometallates.[18-24,25] If HF-rich and $KMnO_4$-rich solutions were used for synthesis of $BaTiF_6:Mn^{4+}$, phase K_2SiF_6 and MnO_2 should exist in the products. As we studied, the obtained MnO_2 are uniform nanowires, which cannot be observed in XRD of crystals in micrometer level.[27] The trace phase of K_2SiF_6 or $BaSiF_6$ may go beyond the limitation of measurement. But trace of $K_2SiF_6:Mn^{4+}$ or $BaSiF_6:Mn^{4+}$ in the sample $BaTiF_6$ may make the sample show red luminescence that can be detectable by photoluminescence (PL) measurements. Therefore, it is desirable to develop a simple and economical method for synthesis of pure phased red Mn^{4+} doped phosphors with excellent properties.

Herein, we report on an efficient one-step method including hydrothermal and etching for the preparation of a red phosphor $BaTiF_6:Mn^{4+}$ with different micro morphologies from TiO_2 and $Ti(OC_4H_9)_4$. The effects of starting materials and reaction temperature on the red phosphor $BaTiF_6:Mn^{4+}$ have been investigated in details. The optimum concentration of $KMnO_4$ for preparing $BaTiF_6:Mn^{4+}$ is 1.5 mmol/L which is much lower than those applied in previous works (200 mmol/L).[18-24] The possible growth mechanism of red phosphor $BaTiF_6:Mn^{4+}$ with different morphologies has been discussed.

2. Experimental

2.1. Synthesis

The red phosphor $BaTiF_6:Mn^{4+}$ samples were prepared via a one-step method including hydrothermal and etching in a solution containing HF and $KMnO_4$. All the starting materials were purchased from Sinopharm Chemical Reagent Co. Ltd., Shanghai, China. In a typical process for synthesizing the red phosphor $BaTiF_6:Mn^{4+}$, the starting materials BaF_2 (A. R.), n-titanium butoxide $Ti(OC_4H_9)_4$ (A. R.), $KMnO_4$ (A. R.), HF (wt.40%), and distilled water were mixed thoroughly in a Teflon-cup. The molar ratios of BaF_2 and $Ti(OC_4H_9)_4$ were kept at 1:1. The concentration of HF was kept at 10 wt.% in all reactions. The concentration of $KMnO_4$ in the system was varied between 0.5 and 2.5 mmol/L. Hydrolyzing of titanium butoxide occurred in the mixing process. For comparison, commercially purchased TiO_2 (A. R.) was used for source of titanium in $BaTiF_6:Mn^{4+}$ in some cases. The Teflon vessel containing the suspension was closed in a stainless steel autoclave, and kept at 120 °C for 20 h. After reaction, the autoclave was then cooled naturally to room temperature. The resulting white solid products were filtered, washed with distilled water, and dried under vacuum at room temperature for 24 h.

2.2. Characterization

X-ray powder diffraction (XRD) patterns of the as-prepared samples were examined using a diffractometer (D8 Advance, Bruker, Germany) equipped with graphite monochromatized Cu Kα radiation (λ=0.15406 nm) as the x-ray source. Identifications of phases were made using standard JCPDS files. The morphologies of the samples were studied by a field emission scanning electron microscopy (FE-SEM) on Nova NanoSEM 200 scanning electron microscope (FEI Inc.) with an attached energy-dispersive x-ray spectrum (EDS). UV-vis reflectance spectra were recorded on a Shimadzu UV-1800 spectrometer with a resolution of 1.0 nm. Photoluminescence (PL) spectra were recorded on FluoroMax-4 spectrofluorometer (Horiba Jobin Yvon Inc.) with a 150 W xenon lamp at room temperature.

3. Results and discussion

3.1. Composition, morphology, and thermal stability

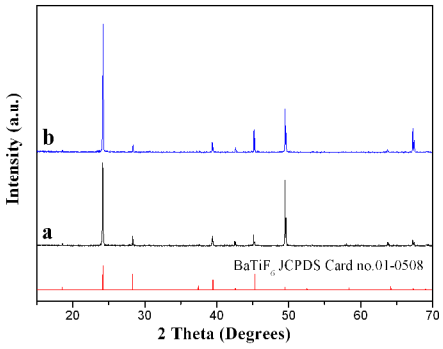

Fig. 1 XRD patterns of the as-synthesized red phosphors $BaTiF_6:Mn^{4+}$ obtained from starting materials BaF_2, HF, $KMnO_4$ and (a) $Ti(OC_4H_9)_4$ and (b)TiO_2 at 120 °C for 20 h.

The crystal phases of the as-synthesized red phosphors $BaTiF_6:Mn^{4+}$ have been determined by XRD as shown in Fig. 1. The XRD patterns of the phosphors $BaTiF_6:Mn^{4+}$ from both TiO_2 and $Ti(OC_4H_9)_4$ are almost identical. All the diffraction peaks can be indexed to pure rhombohedral structure of $BaTiF_6$ with space group R-3m (166) and cell volume 340.91 $Å^3$ (JCPDS card no. 01-0508). The sharp diffraction peaks indicate that $BaTiF_6$ is crystallized in large size. No obvious phases of manganese oxides is detected, which indicates Mn^{4+} ions occupy octahedral Ti^{4+} sites due to the similar ionic radii and charge balance. The XRD patterns of samples prepared at different temperatures are shown in Fig. 1S in ESI† and pure $BaTiF_6$ phases can be obtained from by hydrothermal method at a temperature higher than 80 °C. The diffraction peaks increase in intensity with further increase of reaction temperature, which results in higher luminescence intensity. We could not obtain red phosphor $BaTiF_6:Mn^{4+}$ by repeating two-step experiments for preparing $BaTiF_6:Mn^{4+}$ reported.[26] The unclear phases may be attributed to $BaSiF_6$ produced by H_2SiF_6 and BaF_2, or starting materials which is not soluble at room temperature in previous work.[26] It is tentatively believed that the reaction rates of etching and redox are significant for Mn^{4+} doping in hexafluorometallates according to extensive research on synthesis in our work. The reaction mechanism responsible for formation of $BaTiF_6:Mn^{4+}$ may be due to simultaneous reactions of etching and redox expressed as the following equations:

$$TiO_2 + BaF_2 + 4HF \rightarrow BaTiF_6\downarrow + 2H_2O \quad (1)$$

$$4KMnO_4 + 2BaF_2 + 20HF \rightarrow 2K_2MnF_6 + 2BaMnF_6 + 10H_2O + 3O_2 \quad (2)$$

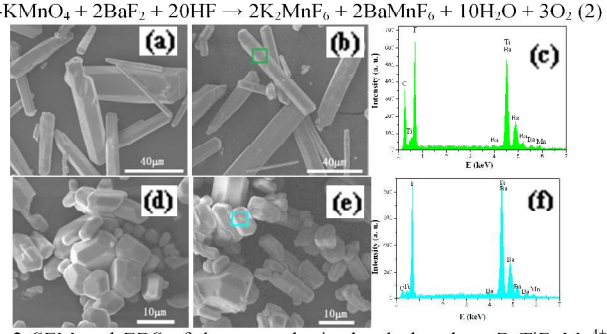

Fig. 2 SEM and EDS of the as-synthesized red phosphors $BaTiF_6:Mn^{4+}$ obtained from starting materials BaF_2, HF, $KMnO_4$ and (a-c) TiO_2 and (d-f) $Ti(OC_4H_9)_4$ at 120 °C for 20 h.

SEM and EDS of the as-synthesized red phosphors $BaTiF_6:Mn^{4+}$ obtained from TiO_2 and $Ti(OC_4H_9)_4$ are shown in Fig. 2. Rod shaped crystals with diameter about 10 μm and length at 70 μm are obtained from TiO_2 (Fig. 3a,b) and polyhedral particles of $BaTiF_6:Mn^{4+}$ with diameters at 5~10 μm are obtained from $Ti(OC_4H_9)_4$ (Fig. 3d,e). The morphologies of $BaTiF_6:Mn^{4+}$ from different titanium sources are different. We measured XRD and SEM of starting materials BaF_2, TiO_2 commercially obtained, and TiO_2 nanoparticles hydrolyzed from $Ti(OC_4H_9)_4$ as shown in Fig. 2S in ESI†. Fresh hydrolyzed TiO_2 nanoparticles have much larger surface area and higher chemical reactivity than commercially obtained TiO_2 micro-particles. The growth rate of $BaTiF_6:Mn^{4+}$ obtained from TiO_2 nanoparticles is faster than that from TiO_2 micro-particles. The faster growth rate of $BaTiF_6:Mn^{4+}$ obtained from TiO_2 nanoparticles leads to small size of crystals. Obviously, the morphologies of $BaTiF_6:Mn^{4+}$ are quite different from those of starting materials, which indicates the $BaTiF_6$ crystals in our experiments are not grown in in-situ of starting materials. The growth process of $BaTiF_6$ crystal is therefore effective in controlling the particle size and morphologies of $BaTiF_6:Mn^{4+}$. To provide further insight into the composition

and structure of the as-prepared red phosphors from TiO_2 and $Ti(OC_4H_9)_4$, the micro rods and polyhedral particles are analyzed by EDS mapping measurements (Fig. 2c,f). EDS results indicate both crystals are composed of Ba, Ti, F and Mn. The molecule ratio of Mn/Ti is less than 0.25 mol%. Element C in the spectrum is from the grids. XPS spectrum of the sample obtained from $Ti(OC_4H_9)_4$ also indicates the composition of $BaTiF_6:Mn^{4+}$ as shown in Fig. S3 in ESI† that is consistent with the experimental results in EDS. Fig. S4 in ESI† exhibits SEM images of $BaTiF_6:Mn^{4+}$ prepared from TiO_2 and $Ti(OC_4H_9)_4$ at different temperatures. The sample prepared from $Ti(OC_4H_9)_4$ at 80 °C is composed of irregular particles with different sizes and the particles grow with increasing temperature. Well dispersed and uniform polyhedral particles with diameter within 10 μm are obtained from $Ti(OC_4H_9)_4$ at 240 °C. Increasing the reaction time does not seem to give significant changes in morphology of micro rods of $BaTiF_6:Mn^{4+}$ formed from TiO_2.

The thermal behavior of the red phosphor $BaTiF_6:Mn^{4+}$ has been measured by TG-DSC analysis (Fig. S5 in ESI†). Weight loss (~5%) on TG and an endothermic peak on DSC curve at temperature lower than 100 °C is owing to the dehydration of water molecule absorbed on the crystal surfaces. The crystals of $BaTiF_6:Mn^{4+}$ keep constant weight below 390 °C. An endothermic peak at 445 °C indicates that the $BaTiF_6:Mn^{4+}$ crystals begin to decompose with the temperature increasing further.

3.2. Optical properties and application in WLEDs

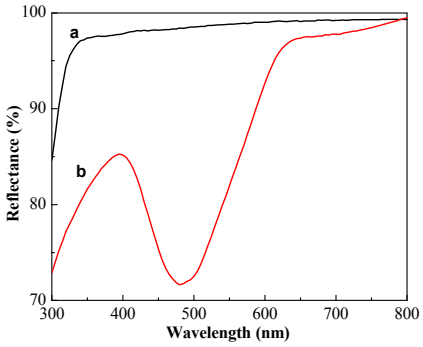

Fig. 3 Diffuse reflection spectra of (a) undoped $BaTiF_6$ and (b) red phosphors $BaTiF_6:Mn^{4+}$.

The vibrational structure of $BaTiF_6:Mn^{4+}$ and undoped $BaTiF_6$ are studied by Raman spectroscopy recorded at room temperature as shown in Fig. S6 in ESI†. The bands at low frequencies, up to approximately 600 cm^{-1}, are ascribed to the Raman modes and agree with the characteristic Raman vibrations of Ti-F stretching modes in group $[TiF_6]^{2-}$.[22,28] The Raman peaks of $BaTiF_6:Mn^{4+}$ attributed to Ti-F stretching modes shift to lower wavenumbers compared to undoped $BaTiF_6$ due to a slight change in the lattice symmetry by substituting Ti^{4+} with Mn^{4+}. The maximum phonon energies of both $BaTiF_6:Mn^{4+}$ and $BaTiF_6$ are at 625.5 cm^{-1}, which is much lower than those in oxides.[29]

Fig. 3 exhibits diffuse reflection spectra of undoped $BaTiF_6$ and red phosphors $BaTiF_6:Mn^{4+}$. It is observed that the $BaTiF_6$ host demonstrates little absorption in visible region. A strong absorption is observed in blue region with a maximum at 470 nm in the curve of red phosphors $BaTiF_6:Mn^{4+}$, which is indicative of its potential application in blue semiconductor chips.

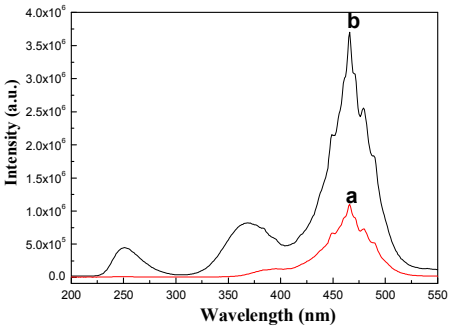

Fig. 4 Excitation spectra (monitored at 632 nm) of the as-synthesized red phosphor $BaTiF_6:Mn^{4+}$ obtained from starting materials BaF_2, HF, $KMnO_4$ and (a) TiO_2 and (b) $Ti(OC_4H_9)_4$ at 120 °C for 20 h.

The crystal structure of $BaTiF_6$ belongs to rhombohedral structure with the lattice constant of a=b=7.368 Å, c=7.252 Å. The Ti atom is sixfold coordinated by six F ions. as shown in Fig. S7 in ESI†. Mn^{4+} ions substitute octahedral Ti^{4+} ions sites in $BaTiF_6$ based on the similar ionic radii and charge balance. The optical properties of phosphor samples $BaTiF_6:Mn^{4+}$ obtained from TiO_2 and $Ti(OC_4H_9)_4$ are comparatively studied as shown in Fig. 4. Both excitation spectra have a strong broad and maximum absorption in blue region, which are ascribed to spin-allowed and parity-forbidden transitions $^4A_2$ - $^4T_1$ of Mn^{4+}. The absorption in blue region is indicative of potential application of the phosphor $BaTiF_6:Mn^{4+}$ in blue InGaN chips. The excitation spectrum of $BaTiF_6:Mn^{4+}$ obtained from $Ti(OC_4H_9)_4$ have two bands in UV region, which are attributed to transitions from split $^4T_2$ levels.

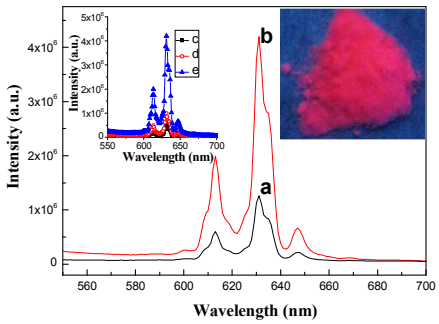

Fig. 5 Emission spectra (excited at 460 nm) of the as-synthesized red phosphor $BaTiF_6:Mn^{4+}$ obtained from starting materials BaF_2, HF, $KMnO_4$, (a) TiO_2, and (b) $Ti(OC_4H_9)_4$ at 120 °C for 20 h. Insert: emission spectra of the as-synthesized red phosphor $BaTiF_6:Mn^{4+}$ obtained from starting materials BaF_2, HF, $KMnO_4$ and $Ti(OC_4H_9)_4$ under excitation at (c) 250 nm, (d) 360 nm, and (e) 466 nm.

The as-prepared phosphor $BaTiF_6:Mn^{4+}$ emits red luminescence under excitation of blue light (Fig. 5 insert). As shown in Fig. 5, the emission spectra of $BaTiF_6:Mn^{4+}$ are composed of three bands with maximum at 613 nm, 630 nm, and 647 nm, which are attributed to transitions between vibronic levels of ^2E and $^4A_2$ of Mn^{4+}. The luminescence of $BaTiF_6:Mn^{4+}$ obtained from $Ti(OC_4H_9)_4$ is more intense than that from TiO_2 under identical experimental conditions, which may be due to the nanosized TiO_2 hydrolyzed from $Ti(OC_4H_9)_4$ is helpful to Mn^{4+} doping in TiF_6^{2-} structure. The emission spectra (Fig. 5 insert) of the as-synthesized red phosphor $BaTiF_6:Mn^{4+}$ excited at 250 nm, 360 nm, and 466 nm have identical spectral features, which indicates only one kind of Ti^{4+} site in TiF_6^{2-} that Mn^{4+} can occupies.

The influence of reaction temperature and concentration of

$KMnO_4$ on luminescence of red phosphor $BaTiF_6:Mn^{4+}$ have been investigated (Fig. S8 and Fig. S9 in ESI†). The emission intensity can be improved by increasing reaction temperature from 80 °C to 240 °C, which is due to improved crystallization at higher temperature. The optimized concentration of $KMnO_4$ in reaction system is 1.5 mmol/L that is much lower than those (200 mmol/L) in reported works.[18-24] Though the concentration of $KMnO_4$ is low enough, the majority of $[MnO_4]^-$ cannot be reduced into Mn^{4+} and enter $[TiF_6]^{2-}$ to form $[MnF_6]^{2-}$ according to EDS and XPS data. The solution becomes purple while adding $NaBiO_3$ solution, which indicates some of $[MnO_4]^-$ may be changed into Mn^{2+} left in the solution. In our work, MnO_2 can be detected while the concentration of $KMnO_4$ as high as those in references.[18-24,27]

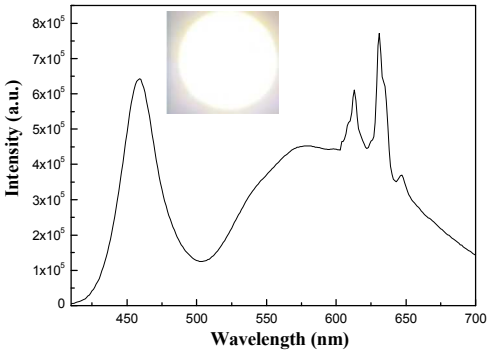

Fig. 6 White luminescence spectra of WLED fabricated with blue GaN chip, yellow phosphor YAG:Ce, and red phosphor $BaTiF_6:Mn^{4+}$. Insert: image of WLED under current of 20 mA.

The LEDs fabricated with blue InGaN chip, yellow phosphor YAG:Ce and red phosphor $BaTiF_6:Mn^{4+}$ exhibits bright "warm" white light under current of 20 mA (Fig. 6). The WLED possesses a color rendering index of 93.13, color coordinates of (0.366, 0.3331) at color temperature 4073.1 K, and an efficiency of 121 lm/W (Table 1 in ESI†).

Conclusions

A red phosphor $BaTiF_6:Mn^{4+}$ with morphologies of micro-rods and polyhedral particles have been prepared from TiO_2 and $Ti(OC_4H_9)_4$ by a one-step method including hydrothermal and etching. The $BaTiF_6$ crystal in our experiments are not grown in in-situ of starting materials and the growth process of $BaTiF_6$ crystal is effective in controlling the particle size and morphologies of $BaTiF_6:Mn^{4+}$. There are only one kind of Ti^{4+} site in TiF_6^{2-} that Mn^{4+} can occupies. The optimal concentration of $KMnO_4$ in reaction system for synthesis of $BaTiF_6:Mn^{4+}$ is 1.5 mmol/L, which is much lower than those in reported works. The $BaTiF_6:Mn^{4+}$ based WLED exhibits "warm" white light with a color rendering index of 93.13.

This research was jointly supported by Chinese NSF (Grant no.51102185), Zhejiang Provincial Science and Technology (Grant no.KZ1209005) and, Qianjiang talents project (Grant no. QJD1302005).

Notes and references

Address, Nanomaterials and Chemistry Key Laboratory, Faculty of Chemistry and Materials Engineering, Wenzhou University, Zhejiang Province, Wenzhou 325027, P. R. China. Tel. & Fax: (+86) 577-8837-3017. E-mail:yxpan8@gmail.com; smhuang@wzu.edu.cn

†Electronic Supplementary Information (ESI) available: XRD of samples obtained at different temperatures, TG-DSC, XPS and Raman spectra of $BaTiF_6:Mn^{4+}$, XRD patterns and SEM images of starting materials, SEM of $BaTiF_6:Mn^{4+}$ prepared at different temperatures, the structure projection of $BaTiF_6:Mn^{4+}$, dependence of emission spectra of $BaTiF_6:Mn^{4+}$ on reaction temperature and concentration of $KMnO_4$, the performance parameters of the white LEDs coated with red phosphor $BaTiF_6:Mn^{4+}$.See DOI: 10.1039/b000000x/

1 M. M. Jiao, Y. C. Jia, W. Lu, W. Z. Lv, Q. Zhao, B. Q. Shao and H. P You, *J. Mater. Chem.* C., 2014, **2**, 90.
2 C. Y. Liu, Z. G. Xia, Z. P. Lian, J. Zhou and Q. F. Yan, *J. Mater. Chem. C.*, 2013, **1**, 7139.
3 J. K. Park, S. J. Lee and Y. J. Kim, *Cryst. Growth Des.*, 2013, **13 (12)**, 5204.
4 Y. Q. Li, N. Hirosaki, R. J. Xie, T. Takeda and M. Mitomo, *Chem. Mater.,* 2008, **20**, 6704.
5 Z. Y. Zhao, Z.G. Yang, Y. R. Shi, C. Wang, B. T. Liu, G. Zhu and Y. H. Wang, *J. Mater. Chem. C.*, 2013, **1**, 1407.
6 K. Y. Jung, H. W Lee and H.K. Jung, *Chem. Mater*., 2006, **18**, 2249.
7 C. Hecht, F. Stadler, P. J. Schmidt, J. r. S. auf der G¨unne, V. Baumann and W. Schnick, *Chem. Mater*., 2009, **21**, 1595.
8 A. A. Setlur, E. V. Radkov, C. S. Henderson, J. H. Her, A. M. Srivastava, N. Karkada, M. S. Kishore, N. P. Kumar, D. Aesram, A. Deshpande, B. Kolodin, L. S. Grigorov and U. Happek, *Chem. Mater*., 2010, **22**, 4076.
9 Q. H. Zeng, P. He, M. Pang, H. B. Liang, M. L. Gong and Q., Su, *Solid State Commun.,* 2009, **149**, 880.
10 M. Yamada, T. Naitou K. Izuno, H. Tamaki,Y. Murazaki, M. Kameshima and T. Mukai, *Jpn. J. Appl. Phys*., 2003, **42**, 20.
11 J. Yu, K. K. Huang, L. Yuan and S. H. Feng, *New J. Chem*., 2013, DOI: **10**.1039/c3NJ01096a
12 A. P. Jadhav, A. U. Pawar, U. Palc and Y. S. Kang, *J. Mater. Chem. C.*, 2014, DOI: **10**.1039/c3tc31939c.
13 L. Zhang, Z. Lu, P. D. Han, L. X. Wang and Q. T. Zhang, *J. Mater. Chem. C.*, 2013, **1**, 54.
14 J. C. Zhang, Y. Z. Long, H. D. Zhang, B. Sun, W. P. Han and X. Y. Sun, *J. Mater. Chem. C.*, 2014, DOI: **10**.1039/c3tc31798f.
15 J. Lin, Y. Huang, J. Mi, X.H. Zhang, Z. M. Lu, X. W. Xu, Y. Fan, J. Zou and C. C. Tang, *Nanotech.*, 2013, **24**, 405701.
16 W. B. Park, S. P. Singh, C. Yoon and K. S. Sohn, *J. Mater. Chem*., 2012, **22**, 14068.
17 J. Park, S. J. Lee and Y. J. Kim, Crystal. Growth Design., 2013, DOI:**10**.1021/cg4.
18 C. X. Liao, R.P. Cao, Z. J. Ma, Y. Li, G. P. Dong, K. N. Sharafudeen and J. R. Qiu, *J. Am. Chem. Soc.*, 2013, **10**, 12533.
19 T. Takahashi and S. Adachi, *Electrochem. Solid-State Lett.,* 2009,**12,** J69.
20 T. Takahashi and S. Adachi, *J. Electrochem. Soc.,* 2008, **155**, E183.
21 S. Adachi and T. Takahashi, *J. Appl. Phys*., 2009, **106**, 013516.
22 Y. K. Xu and S. Adachi, *J. Electrochem. Soc.,* 2011, **158**, J58.
23 R. Kasa and S. Adachi, *J. Appl. Phys*., 2012, **112**, 01350.
24 Y. K. Xu and S. Adachi, *J. Appl. Phys.,* 2009, **105**, 013525.
25 E. V. Radkov, L. S. Grigorov, A. A. Setlur and A. M. Srivastava, US Patent: 7497973 B2..

26 D. Sekiguchi and S. Adachi, *ECS J. Solid State Sci. Tech.*, 2014, **3**, R60.
27 X. Y. Jiang, Y. X. Pan, S. M. Huang, X. A. Chen, J. G. Wang and G. K. Liu, *J. Mater. Chem. C*, 2014, **2,** 2301..
28 R. L. Brutchey, E. S. Yoo. D and E. Morse, *J. Am. Chem. Soc*., 2006, **128**, 10288.
29 B. Q. Shao, Q. Zhao, N. Guo, Y. C. Jia, W. Z. Lv, M. M. Jiao, Wei. Lu and H. P. You, *Cryst. Eng. Commun.*, 2013, **15**, 5776.

A graphical and textual abstract

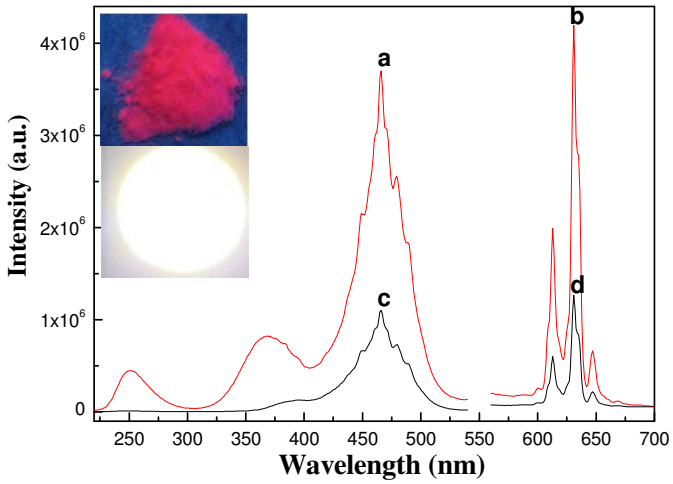

Red phosphors $BaTiF_6:Mn^{4+}$ were obtained by etching (a,b) $Ti(OC_4H_9)_4$ and (c,d) TiO_2 with BaF_2 in HF and $KMnO_4$ solution. The WLED fabricated with $BaTiF_6:Mn^{4+}$ exhibits "warm" white light with a color rendering index of 93.13.